Synthesis of carbon nanotubes over nickel–iron catalysts supported on alumina under controlled conditions

A.K.M. Fazle Kibria, Y.H. Mo and K.S. Nahm *

School of Chemical Engineering and Technology, Chonbuk National University, Chonju 561-756, Republic of Korea
E-mail: nahmks@moak.chonbuk.ac.kr

Received 8 September 2000; accepted 28 November 2000

Carbon nanotubes (CNTs) were synthesized by catalytic decomposition of acetylene over Fe, Ni and Fe–Ni catalysts supported on alumina. The growth of CNTs was carried out at various reaction conditions. The growth density and diameter of CNTs could be controlled by varying the catalyst composition and the growth parameters. The growth density of CNTs increased with increasing the activation time of catalysts in H_2 atmosphere and/or decreasing acetylene concentration. At 600 °C, higher density of CNTs was observed at 60 min for higher Fe containing catalyst, whereas at 90 min for higher Ni containing catalyst. The growth density of CNTs highly increased with increasing reaction time from 30 to 60 min. For all the catalysts, the diameter of CNTs decreased with increasing growth time further mainly due to hydrogen etching. Bimetallic catalysts produced narrower diameter CNTs than single metal catalysts. The growth of CNTs followed the tip growth mode and the CNTs were multi-walled CNTs.

KEY WORDS: carbon nanotubes; Fe–Ni/Al_2O_3 catalyst; acetylene; growth density

1. Introduction

The extraordinary properties of carbon nanotubes (CNTs) such as a metal, semiconductor and superconductor, and in parallel the hydrogen storage capability of CNTs and carbon nanofibers (CNFs) have produced much interest in searching their easier and low-cost synthesis route [1–5]. Recently, research interests have been focused on the catalytic synthesis route where hydrocarbons such as CH_4, C_2H_6, C_2H_4, C_2H_2 and CO are used as the carbon source, and Fe, Ni, Co and Fe–Ni are used as catalysts [6–15]. This synthesis route shows numerous merits over other growth techniques such as arc discharge process [16] and laser ablation method [17]. Besides the purity of product, the large amount of CNTs and CNFs can be grown at moderate temperatures with low cost, and the control of tube structure can be realized by regulating the growth parameters and catalyst composition as well as by modifying the nanomorphology of the catalysts with dispersion of metals on supports [6–14].

Supports like Al_2O_3 and SiO_2 show profound effect on the structural and morphological characteristics of metal particles, which determine physical properties of grown CNTs and CNFs [6,8]. Recently, the catalytic activity of iron, nickel and cobalt supported on Al_2O_3 and SiO_2 has been investigated to see the effect of the supports [6,9–11,14]. Compared with single metal supported catalysts, however, it has been rarely reported that bimetallic catalysts were employed to grow CNTs. Baker et al. [12,13] extensively studied the activity of the unsupported Fe–Ni catalysts using C_2H_6/H_2, CO/H_2 and $C_2H_4/CO/H_2$, and established that the composition and nature of the bimetallic catalyst in conjunction with the carbon-containing gas and reaction conditions have a dramatic impact on the production and the crystalline perfection of the CNFs. Very recently, remarkably narrow tubular CNFs with various geometries and crystallinities have been observed from the decomposition of CO/H_2 over various compositions of Fe–Ni particles supported on SiO_2 [8]. The CNFs grown on supported and unsupported Fe–Ni catalysts showed very different morphologies because of attaining different arrangement of graphite platelets [8,12,13]. The findings using Fe–Ni/SiO_2 catalysts represented a unique development of catalytic method to synthesize relatively large quantities of CNFs of controlled size in tubular structure. In CH_4/H_2 gas medium, the growth of huge amount of single-wall and multi-wall carbon nanotubes (SWNTs and MWNTs) with a diameter range of 1.5–15 nm has been reported [9] in the mixture of CNTs–Fe–Al_2O_3 composites. The above findings represent that, by varying the catalyst, support, carbon source and reaction conditions, high quality nanotubes can be synthesized for future applications. In this context, the present study aims to synthesize CNTs over Fe, Ni and Fe–Ni catalysts supported on Al_2O_3 using C_2H_2 gas as carbon source and H_2 as the carrier gas. The study also includes the morphological and structural characterization of the grown CNTs.

2. Experimental

We prepared three bimetallic catalysts with different weight proportions of Fe : Ni : Al_2O_3 (30 : 10 : 60, 20 : 20 : 60, 10 : 30 : 60) and two metallic catalysts 40Fe(Ni) : 60Al_2O_3 using an impregnation method. High metal loading was chosen in order to obtain longer catalytic activity. The

* To whom correspondence should be addressed.

1011-372X/01/0200-0229$19.50/0

size of the used α-Al_2O_3 powder was 0.3 μm. To prepare the catalysts, aqueous solutions of $Fe(NO_3)_3{\cdot}9H_2O$ and/or $Ni(NO_3)_2{\cdot}6H_2O$ were mixed each other with Al_2O_3 and stirred for about 1 h at 60 °C. The impregnate was dried in an oven at 100 °C for 12 h, calcined at 400 °C for 4 h and reduced in 100 sccm hydrogen flow at 450 °C for 3 h. The produced supported catalysts were stored in sealed vessels and the nanotubes were synthesized over the catalysts.

The nanotube synthesis was carried out according to the following procedure. Approximately 40 mg of a catalyst sample was uniformly dispersed in the base area of a quartz plate and placed in the central region of a horizontal quartz tube reactor. There, the catalyst was activated at 900 °C in 100 sccm H_2 flow to obtain the best active state, and then the growth of carbon nanotubes was carried out. In order to find out the optimum growth condition, CNTs were grown at temperatures between 500 and 700 °C by flowing 10/100 sccm C_2H_2/H_2 for different time periods. The effect of C_2H_2 concentration on the growth of nanotubes was also investigated. The structure and morphology of the synthesized nanotubes were determined by using scanning electron microscopy (SEM), transmission electron microscopy (TEM) and FT-Raman spectroscopy.

3. Results and discussion

We have first attempted to optimize the catalyst activation condition for the best growth of CNTs. Figure 1 (a), (b) and (c) shows the SEM images for the CNTs grown over the $20Fe:20Ni:60Al_2O_3$ catalyst at 600 °C for 60 min under 10/100 sccm C_2H_2/H_2 flow after activation periods of 5, 30 and 60 min, respectively. With increasing the activation time, the growth density of CNTs gradually increases, whereas the nanotube diameter decreases dramatically. The average diameter of the CNTs grown over 60 min activated catalyst seems to be about 20 nm, which is almost three times narrower than that grown over 30 min activated catalyst. In order to obtain more detailed information on the 60 min grown CNTs, we measured the specific surface area of the 60 min activated catalyst before and after the growth of CNTs by the Brunauer–Emmett–Teller (BET) method using N_2 adsorption at liquid nitrogen temperature which

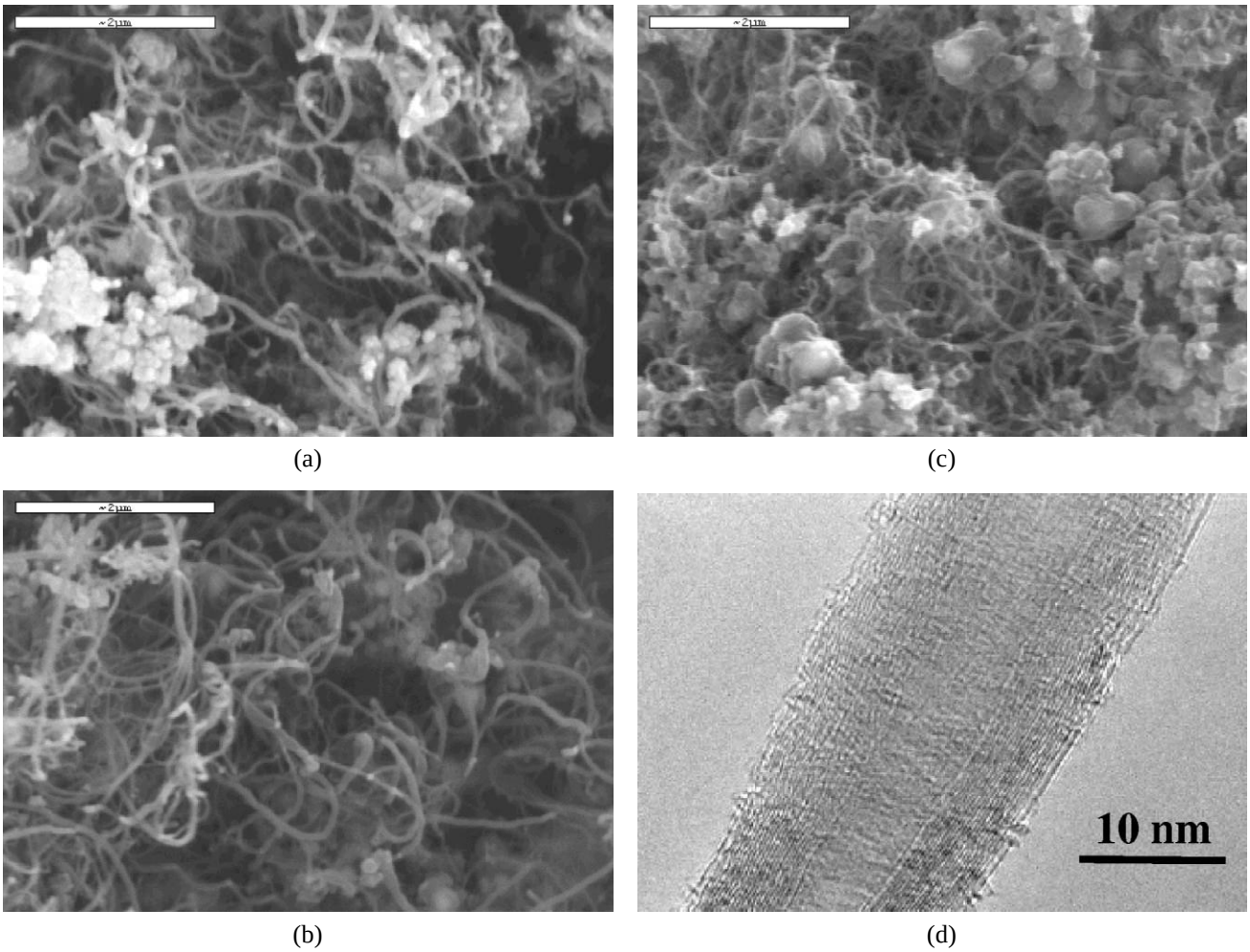

(a) (c)

(b) (d)

Figure 1. SEM images for the CNTs grown over $20Fe:20Ni:60Al_2O_3$ catalyst for 60 min at 600 °C under 10/100 sccm C_2H_2/H_2 flow after activating: (a) 5, (b) 30 and (c) 60 min, and (d) HRTEM image of a CNT of (c).

Peigney et al. [9] employed for their catalyst and grown CNTs. The measured surface areas of the catalyst before and after the growth of CNTs are 191.5 and 290.4 m^2/g, respectively. The increase in surface area about 98.9 m^2/g clearly indicates the growth of CNTs. The measured value corresponds to the surface area of the grown CNTs. We calculated the diameter of the grown CNTs by substituting the surface area of the CNTs into the following equation:

$$D = 4/(dS),$$

where D is the diameter of CNTs, d is the density of the CNTs (2.26 g/cm^3) and S is the surface area of the CNTs. The calculated diameter is 17.9 nm. As CNTs are generates from graphene sheet, for calculations the density of CNTs is generally considered to be that of graphite [18,19] and we also used this value. Figure 1(d) shows a high resolution transmission electron microscopy (HRTEM) image of a CNT taken from figure 1(c). The tube consists of twenty one graphite layers with a hollow center of 6.5 nm. The interlayer spacing between the graphite platelets is 0.34 nm and the diameter of the tube is 20 nm which approximately coincides with the diameter estimated from the SEM image and the diameter calculated from the surface area. The decrease in CNTs diameter with increasing activation time indicates that longer activation time has a profound effect on the growth of very narrow diameter tubes. The activation process might cause the conversion of bulk metal oxides to active metal [8,12] as well as the formation of smaller sized metal crystallites, which may be responsible for the growth of CNTs with narrow diameter because the size of metal particle is a decisive condition for the CNT growth [7,20].

Figure 2 (a), (b) and (c) shows the SEM images for the CNTs grown over the $30Fe:10Ni:60Al_2O_3$ catalyst for 60 min at 500, 600 and 700 °C, respectively, under 10/100 sccm C_2H_2/H_2 flow after activating the catalyst for 60 min. It is seen that the growth of CNTs is observed at 600 and 700 °C, whereas no tubes are grown at 500 °C. The growth density at 600 °C is much higher than that at 700 °C. Additionally, the diameter of the CNTs grown at 600 °C is about three times narrower than that grown at 700 °C. Most of the tubes grown at 600 °C seem to follow stepwise growth, whereas those grown at 700 °C are smooth. However, the above findings inform that it is possible to

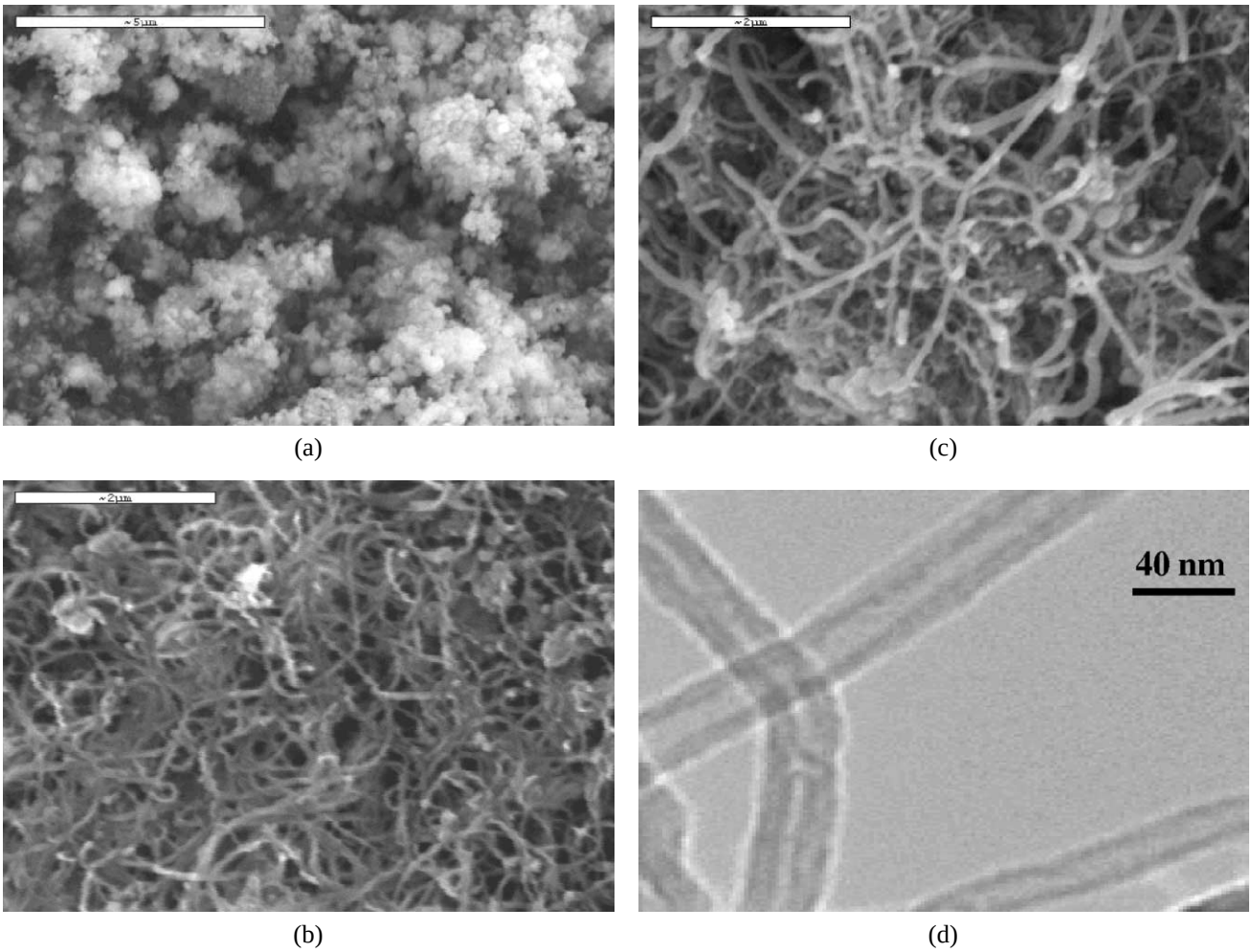

Figure 2. SEM images for the CNTs grown over 60 min activated $30Fe:10Ni:60Al_2O_3$ catalyst for 60 min under 10/100 sccm C_2H_2/H_2 flow at: (a) 500, (b) 600 and (c) 700 °C, and (d) TEM image of CNTs grown at 600 °C (b).

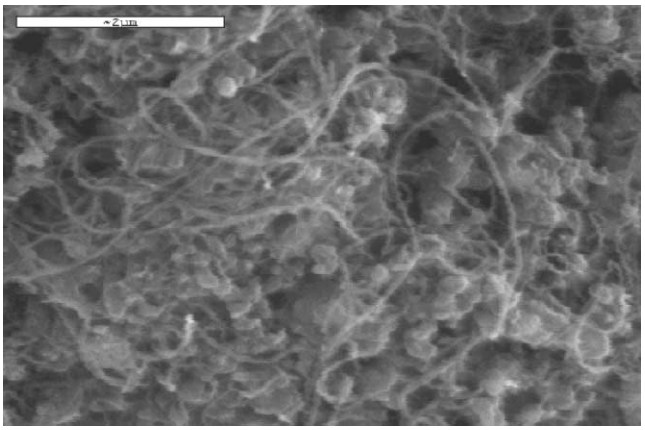

(a)

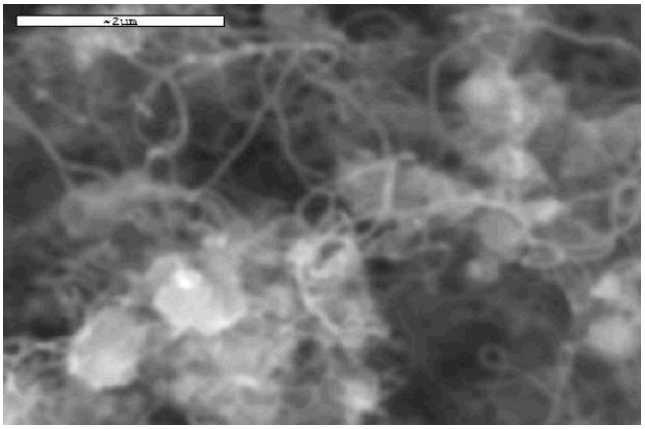

(b)

Figure 3. SEM images for the CNTs grown over 60 min activated $30Fe:10Ni:60Al_2O_3$ catalyst at 600 °C under 10/100 sccm C_2H_2/H_2 flow for: (a) 30 and (b) 90 min.

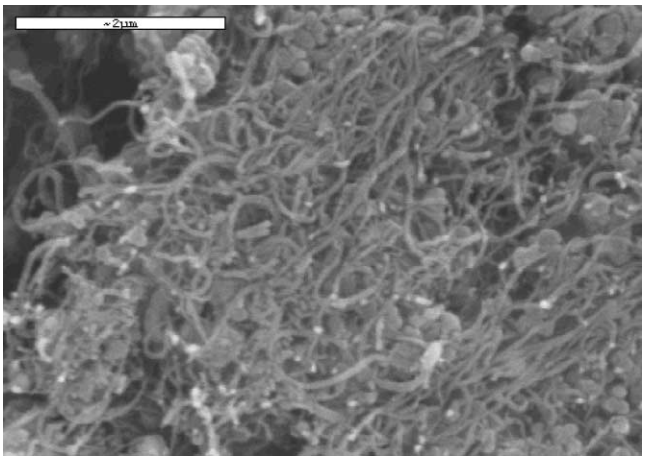

(a)

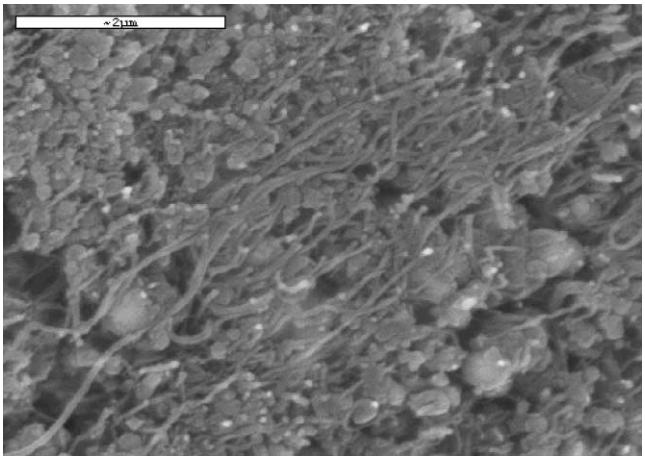

(b)

Figure 4. SEM images for the CNTs grown over 60 min activated $30Fe:10Ni:60Al_2O_3$ catalyst for 60 min at 600 °C under: (a) 20/100 and (b) 30/1000 sccm C_2H_2/H_2 flow.

obtain high density CNTs with narrow diameters by selecting an appropriate reaction temperature. Figure 2(d) shows the TEM image for the CNTs grown at 600 °C (figure 2(b)). The hollow appearance represents the fibrous nature of the grown CNTs and the average diameter of the tubes is about 30 nm, i.e., 10 nm higher than that of the tubes grown on the $20Fe:20Ni:60Al_2O_3$ catalyst under the same experimental condition.

The effect of reaction time on the growth of CNTs over the $30Fe:10Ni:60Al_2O_3$ catalyst was studied using the best catalyst activation period of 60 min and growth temperature of 600 °C under 10/100 sccm C_2H_2/H_2 flow. Figure 3 (a) and (b) shows the SEM images for the CNTs grown for 30 and 90 min, respectively. From figures 3 and 2(b), it may be seen that the growth density and length of CNTs highly increase with increasing the reaction time from 30 to 60 min and then decrease remarkably when increasing the time further up to 90 min. However, the density of CNTs at 90 min growth time is higher than that at 30 min. The decrease of CNT density after 90 min cannot be clearly explained at this point. However, the observation indicates that the reaction time has a remarkable effect on the growth of CNTs and the best growth time is 60 min.

In order to understand the effect of acetylene concentration on the growth of CNTs, the tubes were grown for 60 min at 600 °C under 20 and 30/100 sccm C_2H_2/H_2 flow, respectively, over the $30Fe:10Ni:60Al_2O_3$ catalyst after activating the catalyst for 60 min. The observed SEM photographs are shown in figure 4 (a) and (b) for 20 and 30 sccm C_2H_2, respectively. From figures 4 and 2(b), it may be seen that the tube density decreases with increasing C_2H_2 concentration. However, the quantity of straight tubes with uniform diameters gradually increases with increasing C_2H_2 concentration.

Consequently, the optimum growth condition of CNTs was identified to be the sample activation period of 60 min, reaction time of 60 min, growth temperature of 600 °C and C_2H_2/H_2 flow rate of 10/100 sccm. In order to obtain more clear information for the effect of growth time on the density of CNTs, besides this optimum condition, CNTs were thoroughly grown over all the catalysts after 60 min activation for 5, 30 and 90 min, respectively. The carbon yield (%) is compiled in table 1 as a function of reaction time with some reported data. The carbon yield was calculated by di-

Table 1
Carbon yield (%) as a function of reaction time over the catalysts (present study) with available reported results.

Catalyst	Gas medium	Temp. (°C)	Carbon yield (%)			
			5 min	30 min	60 min	90 min
$40Ni:60Al_2O_3$	C_2H_2/H_2	600	3.09	6.86	11.34	22.83
$40Fe:60Al_2O_3$	C_2H_2/H_2	600	4.48	8.69	16.11	26.55
$20Fe:20Ni:60Al_2O_3$	C_2H_2/H_2	600	10.74	34.48	60.26	74.85
$30Fe:10Ni:60Al_2O_3$	C_2H_2/H_2	600	14.21	46.89	94.19	134.65
$10Fe:30Ni:60Al_2O_3$	C_2H_2/H_2	600	7.55	20.49	39.39	37.18
$Fe:4Ni:95SiO_2$ [8]	CO/H_2	600	–	–	–	105.80
$2.5Fe:2.5Ni:95SiO_2$ [8]	CO/H_2	600	–	–	–	60.20
$4Fe:Ni:95SiO_2$ [8]	CO/H_2	600	–	–	–	24.00
$2.5Fe:97.5SiO_2$ [14]	CH_4/N_2	700	–	29.50	–	–
$Al_{1.9}Fe_{0.1}O_3$ [9]	CH_4/H_2	1050	–	–	2.77	–
$Mg_{0.9}Fe_{0.1}Al_2O_4$ [15]	CH_4/H_2	1070	1.77	–	–	–
$Mg_{0.4}Fe_{0.2}Al_2O_4$ [15]	CH_4/H_2	1070	6.16	–	–	–

Table 2
Diameter (d) of CNTs grown over different supported ($A = Al_2O_3$) catalysts at 600 °C under 10/100 sccm C_2H_2/H_2 flow for 60 min.

	Catalyst				
	40Ni : 60A	20Fe : 20Ni : 60A	30Fe : 20Ni : 60A	10Fe : 30Ni : 60A	40Fe : 60A
d (nm)	55–60	18–20	30	40–45	50–55

viding the increased weight of the catalyst before and after the CNTs growth by the catalyst weight before the growth, as employed by Hernadi et al. [14].

From table 1, it can be seen that for all the catalysts, the carbon yield (%) gradually increases with increasing reaction time except for the $10Fe:30Ni:60Al_2O_3$ catalyst at 90 min. The carbon yields (%) for the bimetallic catalysts are remarkably higher than those for the single metal catalysts. Among the investigated catalysts, the catalytic activity of the $40Ni:60Al_2O_3$ catalyst is the poorest, whereas that of $30Fe:10Ni:60Al_2O_3$ is the best. Compared to the earlier reported data [8,9,14,15], the presently observed results indicate a good activity of the catalysts for the growth of CNTs.

In order to obtain a correlation between the carbon yield (%) and the density of CNTs, SEM measurements were duly carried out. Figure 5 (a), (b) and (c) shows the SEM images for the CNTs grown over $40Fe:60Al_2O_3$, $10Fe:30Ni:40Al_2O_3$ and $40Ni:60Al_2O_3$ catalysts, respectively, at the reaction period of 60 min. It can be seen that high density CNTs are grown over the catalyst surfaces. When comparing the findings regarding the density of CNTs grown for 60 min, as presented in figures 1, 2 and 5, it can be seen that high density CNTs are grown over $30Fe:10Ni:60Al_2O_3$ catalysts (figure 2(b)). This represents that the growth density of CNTs can be fairly well correlated with the carbon yield (%). Although it is clear that the carbon yield (%) gradually increases with increasing reaction time (table 1), the growth rate of CNTs (mg/min g_{cat}) gradually decreases with increasing time. The growth rate is the highest during the 5 min growth time. For example, in the case of $40Ni:60Al_2O_3$, the growth rate after 5 min is 6.18 mg/min g_{cat}, whereas it decreases to 1.89 mg/min g_{cat} after 60 min growth. In the case of $30Fe:10Ni:40Al_2O_3$, this value decreases from 28.42 to 15.69 mg/min g_{cat} for the growth times of 5 and 60 min, respectively. However, the CNTs growth rate over bimetallic catalysts is always higher than over the single metal catalysts.

A close look at the CNTs grown over different catalysts revealed that their diameters are very different. In order to understand the variation of CNTs diameters, the diameters were determined from the surface area measurement, TEM, HRTEM and SEM images for the CNTs grown over different catalysts and are summarized in table 2.

From table 2, it can be seen that the diameters of the CNTs grown over bimetal catalysts are thoroughly smaller than those grown on single metal catalysts. The narrowest diameter tube was grown over the $20Fe:20Ni:60Al_2O_3$ catalyst. It indicates that the diameter of CNT can be controlled using bimetal catalysts.

Figure 6 (a), (b) and (c) shows the SEM images for CNTs grown for 90 min over $40Fe:60Al_2O_3$, $20Fe:20Ni:40Al_2O_3$ and $10Fe:30Ni:40Al_2O_3$ catalysts. It can be seen that in most of the cases, the density of CNTs grown for 90 min is remarkably lower compared with that for 60 min, as was observed for the $30Fe:10Ni:60Al_2O_3$ catalyst (figures 2(b) and 3(b)). Particularly, in the case of a single metal catalyst, the effect of 90 min reaction time on CNT density is severe. In the case of the $40Ni:60Al_2O_3$ catalyst, for example, the growth density was very small (not shown). At this 90 min growth stage, except the activity of the $10Fe:30Ni:40Al_2O_3$ catalyst, there is no evidence showing a correlation between the carbon yield (%) and the density of

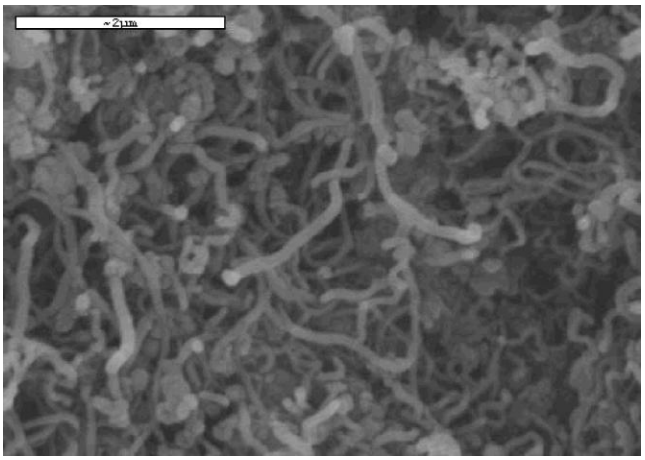

(a)

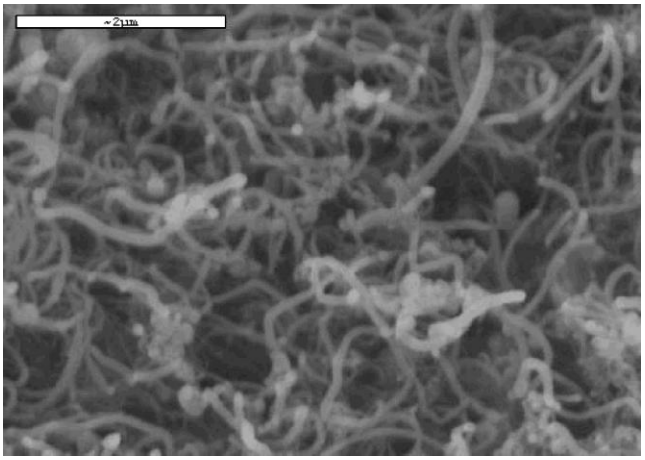

(b)

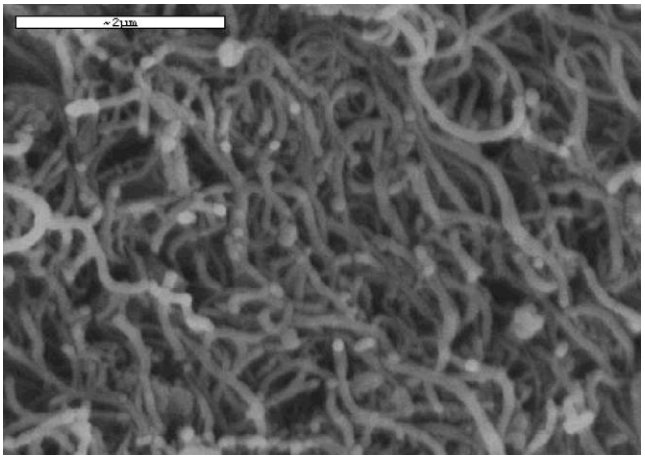

(c)

Figure 5. SEM images for the CNTs grown for 60 min at 600 °C under 10/100 sccm C_2H_2/H_2 flow after 60 min sample activation over: (a) $40Fe:60Al_2O_3$, (b) $10Fe:30Ni:60Al_2O_3$ and (c) $40Ni:60Al_2O_3$ catalysts.

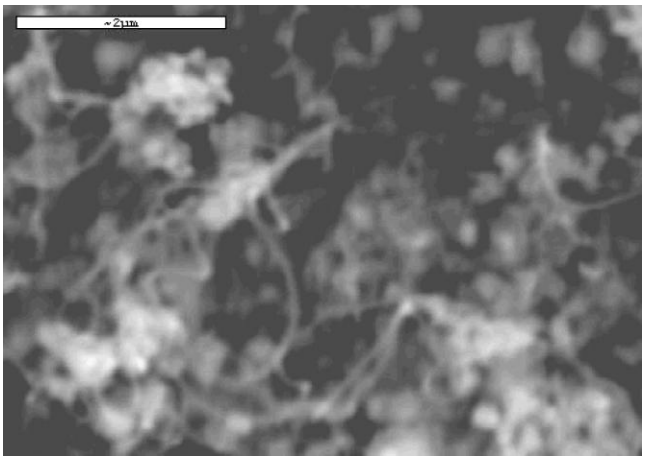

(a)

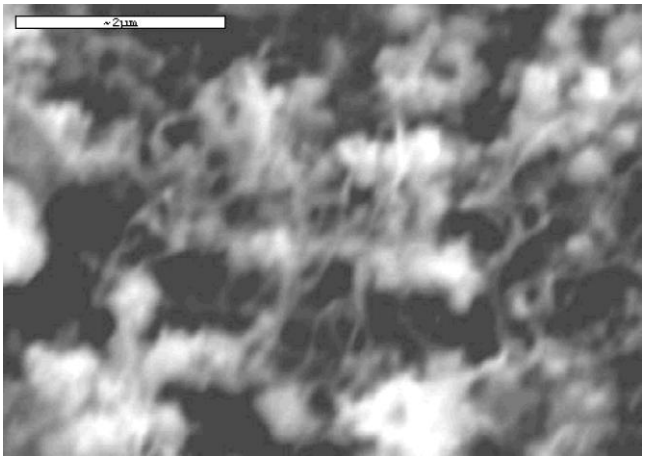

(b)

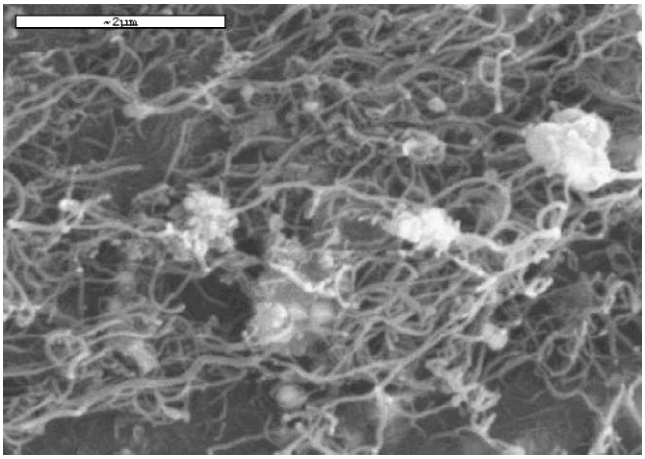

(c)

Figure 6. SEM images for the CNTs grown for 90 min at 600 °C under 10/100 sccm C_2H_2/H_2 flow after 60 min activation over: (a) $40Fe:60Al_2O_3$, (b) $20Fe:20Ni:60Al_2O_3$ and (b) $10Fe:30Ni:60Al_2O_3$ catalysts.

CNTs for all the catalysts. Two factors of the loss of CNTs and gain of carbon yield (%) occurred at the same time.

It is well known that the dissociative chemisorption of hydrocarbons occurs on a particular set of crystallographic faces of the catalyst particle and this step follows carbon dissolution and diffusion through the particle and finally precipitation on a different set of faces to form a tubular structure [8]. If the crystallographic faces for the CNTs forma-

tion are deactivated then only deposition of carbon can be achieved. In the present case, we speculate that the increase in carbon yield (%) during the period of 60–90 min occurs probably due to a deactivation phenomenon. This type of deactivation occurs when the formation of amorphous carbon predominates. It reduces the diffusion rate of carbon source gas to the catalyst and produces remarkably when CNT growth time becomes longer [11,21]. Anderson and Rodriguez [8] have reported 58% amorphous carbon formation in the growth of CNFs over a $Fe:4Ni:95SiO_2$ catalyst for 90 min.

In the present case, the increase of CNT density up to 60 min growth time represents the better activity of the catalysts (table 1). However, the decrease of CNT density and diameter at 90 min indicates that there might be some other factors that have high impacts on the growth of nanotubes. The most probable effect might be hydrogen etching. Other factor such as the loss of preferential sites of one metal during extended period of reaction time cannot be considered because the effect should also have been observed in case of single metal catalysts [8]. Recently, Choi et al. [22] have investigated the hydrogen etching effect on the diameter and length of CNTs grown over nickel thin films under CH_4/H_2 media when increasing the reaction time. In this case, the nanotube diameter decreased almost in a linear fashion with time, for example, from 70 to 20 nm when extending the growth time from 50 to 100 min. For lower hydrogen concentrations, however, the etching effect significantly decreased. Tsai et al. [23] have reported that highly concentrated hydrogen plasma and highly negative bias voltage to the substrate effectively etches the randomly oriented CNTs. In the present case, high hydrogen concentration probably imparted severe etching effect. However, this etching behavior indicates that smaller diameters of CNTs can be synthesized by controlling reaction time.

In order to confirm whether the density and diameter of the nanotube decreased due to the hydrogen etching, alternative growth studies were carried out over the $30Fe:10Ni:60Al_2O_3$ catalyst under 10/100 sccm C_2H_2/N_2 flow for the reaction periods of 60 and 90 min, respectively. The observed SEM images for the grown nanotubes are shown in figure 7 (a) and (b), respectively. The density of CNTs grown for 60 min is much higher than that for 90 min, but the average diameter of CNTs increases with the growth time. The average diameter seems to be equal to that of the large diameter tubes grown for 60 min. It indicates that the hydrogen etching effect was also important for the CNTs grown for 90 min. However, in this case, only smaller diameter tubes were etched by the hydrogen produced during the decomposition of acetylene as observed by quadrupole mass spectroscopy (QMS) [24]. The decrease of CNT density with the growth time coincides with the findings in the case of C_2H_2/H_2 media.

Figure 8 (a) and (b) shows FT-Raman spectra of CNTs grown over the $10Fe:30Ni:60Al_2O_3$ catalyst for 60 and 90 min (figures 5(b) and 6(c)), respectively, at the excitation wavelength of 1064 nm. The spectra clearly show two strong peaks. Both the peaks at 1593 (figure 8(a)) and 1597 cm^{-1} (figure 8(b)) seem to appear due to the C–C stretching Raman-active E_g modes, indicating the formation of graphitized CNTs [22,25]. The peak at around 1284 cm^{-1}

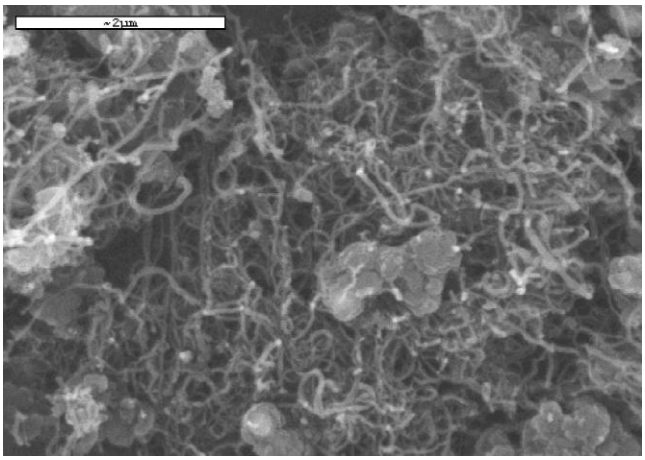

(a)

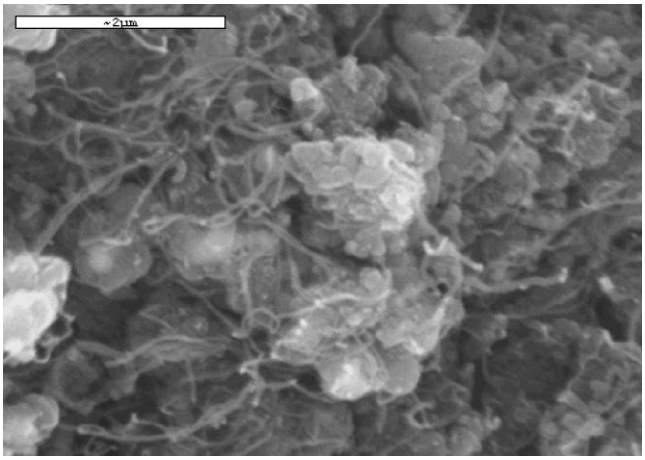

(b)

Figure 7. SEM images for the CNTs grown over 60 min activated $30Fe:10Ni:60Al_2O_3$ catalyst at 600 °C under 10/100 sccm C_2H_2/N_2 flow for: (a) 60 and (b) 90 min.

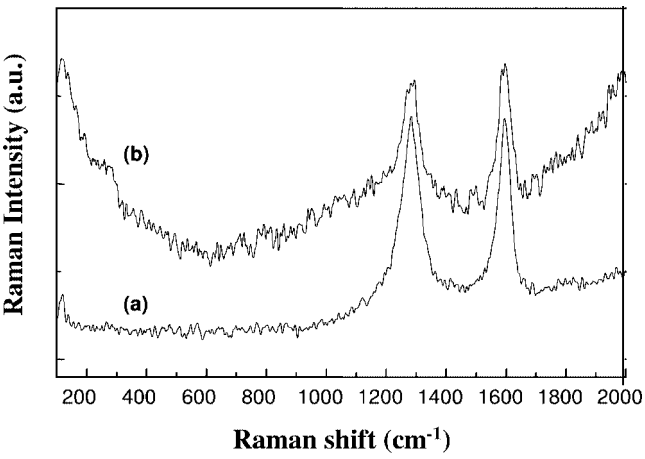

Figure 8. FT-Raman spectra of CNTs grown over $10Fe:30Ni:60Al_2O_3$ catalyst for: (a) 60 and (b) 90 min.

is assigned as the A_g modes of defective carbonaceous particles. It indicates that amorphous carbonaceous particles adhered to CNT walls [22]. It can be seen from the figures that the Raman scattering intensities of E_g mode peaks are comparable to the growth times, whereas that of A_g mode remarkably decreases with increasing growth time. These findings support that amorphous carbon particles adhered to the CNT walls were etched by hydrogen and resulted in the decrease of CNTs diameter as found in SEM images. In comparison with the FT-Raman spectra reported for single-wall carbon nanotubes (SWNTs) [25] and multi-wall carbon nanotubes (MWNTs) [21], the presently observed result coincides with that of MWNTs because the E_g mode peak has no shoulder peaks and no peak for radial breathing mode appears at around 180 cm^{-1}. Moreover, the TEM images of the CNTs grown over $30Fe:10Ni:60Al_2O_3$ and $30Fe:10Ni:60Al_2O_3$ catalysts (figures 1(d) and 2(d)) support the FT-Raman findings that MWNTs were grown in the present study.

In the present study, which examined the effect of bimetal catalysts on the growth of CNTs, probably the CNTs were grown under the catalytic effect of both the metal particles. However, the addition of iron and *vice versa* created dramatically different behavior of CNT growth. In each case, the metal particles can be seen at the tips of the nanotubes as white spots on SEM images. It indicates that CNTs were grown by the tip growth mode. The necessary carbon feedstock supplied from the catalytic decomposition of acetylene, which is dissolved in metals, oversaturated, diffused, and precipitated on the rear surfaces of metal particles generating the CNTs as suggested in previous reports [24,26].

4. Conclusions

In conclusion we have established how to control the growth density and diameter of CNTs by varying catalyst composition as well as by adjusting the catalyst activation time, reaction temperature, reaction time, and carbon source gas concentration.

Acknowledgement

One of us (AKMFK) acknowledges to Korea Science and Engineering Foundation (KOSEF) for a research grant under post-doctoral Fellowship.

References

[1] A. Hassanien, M. Tokumoto, Y. Kumazawa, H. Kataura, Y. Maniwa, S. Suzuki and Y. Achiba, Appl. Phys. Lett. 73 (1998) 3839.
[2] A.Y. Kasumov, R. Deblock, M. Kociak, R. Reulet, H. Bouchiat, I.I. Khodos, Y.B. Gorbatov, V.T. Volkov, C. Journet and M. Burghard, Science 284 (1999) 1508.
[3] C. Nützenadel, A. Züttel, D. Chartouni and L. Schlapbach, Electrochem. Solid State Lett. 2 (1999) 30.
[4] P. Chen, X. Wu, J. Lin and K.L. Tan, Science 285 (1999) 91.
[5] A. Chambers, C. Park, R.T.K. Baker and N.M. Rodriguez, J. Phys. Chem. 102B (1998) 4253.
[6] A. Thaib, G.A. Martin, P. Pinheiro, M.C. Schouler and P. Gadelle, Catal. Lett. 63 (1999) 135.
[7] A. Zhang, C. Li, S. Bao and Q. Xu, Micropor. Mesopor. Mater. 29 (1999) 383.
[8] P.E. Anderson and N.M. Rodriguez, J. Mater. Res. 14 (1999) 2912.
[9] A. Peigney, Ch. Laurent, F. Dobigeon and A. Rousset, J. Mater. Res. 12 (1997) 613.
[10] K. Hernadi, A. Fonseca, P. Piedigrosso, M. Delvaux, J.B. Nagy, D. Bernaerts and J. Riga, Catal. Lett. 48 (1997) 229.
[11] W.Z. Li, S.S. Xie, L.X. Qian, B.H. Chang, B.S. Zou, W.Y. Zhou, R.A. Zhao and G. Wang, Science 274 (1996) 1701.
[12] C. Park and R.T.K. Baker, J. Catal. 190 (2000) 104.
[13] C. Park, N.M. Rodriguez and R.T.K. Baker, J. Catal. 169 (1997) 212.
[14] K. Hernadi, A. Fonseca, J.B. Nagy, D. Bernaerts and A.A. Lucas, Carbon 34 (1996) 1249.
[15] A. Govindaraj, E. Flahaut, Ch. Laurent, A. Peigney, A. Rousset and C.N.R. Rao, J. Mater. Res. 14 (1999) 2567.
[16] K. Tohji, T. Goto, H. Takahashi, Y. Shinoda, N. Shimizu, B. Jeyadevan, I. Matsuoka, Y. Saito, A. Kasuhka, T. Oshuna, K. Hiraga and Y. Nishima, Nature 383 (1996) 679.
[17] A. Thess, R. Lee, P. Nikolaev, H. Dai, P. Petit, J. Robert, C. Xu, Y.H. Lee, S.G. Kim, A.G. Rinzler, D.T. Colbert, G.E. Scuseria, D. Tomanek, J.E. Fischer and R.E. Smalley, Science 273 (1996) 483.
[18] M.S. Dresselhaus, K.A. Williams and P.C. Eklund, Mater. Res. Bull. 24 (1999) 45.
[19] W. Han, S. Fan, Q. Li, W. Liang, B. Gu and D. Yu, Chem. Phys. Lett. 265 (1997) 374.
[20] M. Yudasaka, R. Kikuchi, Y. Ohki, E. Ota and S. Yoshimura, Appl. Phys. Lett. 70 (1997) 1817.
[21] M. Su, B. Zheng and J. Liu, Chem. Phys. Lett. 322 (2000) 321.
[22] Y.C. Choi, D.J. Bae, Y.H. Lee, B.S. Lee, I.T. Han, W.B. Choi, N.S. Lee and J.M. Kim, Synth. Met. 108 (2000) 159.
[23] S.H. Tsai, C.W. Chao, C.L. Lee and H.C. Shih, Appl. Phys. Lett. 74 (1999) 3462.
[24] Y.H. Mo, A.K.M.F. Kibria and K.S. Nahm, Synth. Met., in press.
[25] A.M. Rao, E. Richter, S. Bandow, B. Chasc, P.C. Eklund, K.A. Willams, S. Fang, K.R. Subbaswamy, M. Menon, A. Thess, R.E. Smalley, G. Dresselhaus and M.S. Dresselhaus, Science 275 (1997) 187.
[26] S. Amelinckx, X.B. Zhang, D. Bernaters, X.F. Zhang, V. Ivanov and J.B. Nagy, Science 267 (1995) 635.